

INEEL/CON-99-01324
PREPRINT

SCDAP/RELAP5 Modeling of Movement of Melted Material Through Porous Debris in Lower Head

L. J. Siefken
E. A. Harvego

April 2, 2000 – April 6, 2000

8th International Conference on Nuclear
Engineering

This is a preprint of a paper intended for publication in a journal or proceedings. Since changes may be made before publication, this preprint should not be cited or reproduced without permission of the author.

This document was prepared as a account of work sponsored by an agency of the United States Government. Neither the United States Government nor any agency thereof, or any of their employees, makes any warranty, expressed or implied, or assumes any legal liability or responsibility for any third party's use, or the results of such use, of any information, apparatus, product or process disclosed in this report, or represents that its use by such third party would not infringe privately owned rights. The views expressed in this paper are not necessarily those of the U.S. Government or the sponsoring agency.

SCDAP/RELAP5 MODELING OF MOVEMENT OF MELTED MATERIAL THROUGH POROUS DEBRIS IN LOWER HEAD

Larry J. Siefken
Idaho National Engineering and
Environmental Laboratory
P. O. Box 1625
Idaho Falls, ID 83415 USA
(208) 526-9319
(208) 526-2930
LJS@INEL.gov

E. A. Harvego
Idaho National Engineering and
Environmental Laboratory
P. O. Box 1625
Idaho Falls, ID 83415 USA
(208) 526-9544
(208) 526-2930
HAE@INEL.gov

ABSTRACT

A model is described for the movement of melted metallic material through a ceramic porous debris bed. The model is designed for the analysis of severe accidents in LWRs, wherein melted core plate material may slump onto the top of a porous bed of relocated core material supported by the lower head. The permeation of the melted core plate material into the porous debris bed influences the heatup of the debris bed and the heatup of the lower head supporting the debris. A model for mass transport of melted metallic material is applied that includes terms for viscosity and turbulence but neglects inertial and capillary terms because of their small value relative to gravity and viscous terms in the momentum equation. The relative permeability and passability of the porous debris are calculated as functions of debris porosity, particle size, and effective saturation. An iterative numerical solution is used to solve the set of nonlinear equations for mass transport. The effective thermal conductivity of the debris is calculated as a function of porosity, particle size, and saturation. The model integrates the equations for mass transport with a model for the two-dimensional conduction of heat through porous debris. The integrated model has been implemented into the SCDAP/RELAP5 code for the analysis of the integrity of LWR lower heads during severe accidents. The results of the model indicate that melted core plate material may permeate to near the bottom of a 1 m deep hot porous debris bed supported by the lower head. The presence of the relocated core plate material was calculated to cause a 12% increase in the heat flux on the external surface of the lower head.

INTRODUCTION

In the event of a severe accident in a Light Water Reactor (LWR), particles of a ceramic mixture of UO_2 and ZrO_2 may stack in the lower head of the reactor vessel and form a porous debris bed. The context of the porous debris bed is shown in

Figure 1. A porous debris such as that shown in Figure 1 may

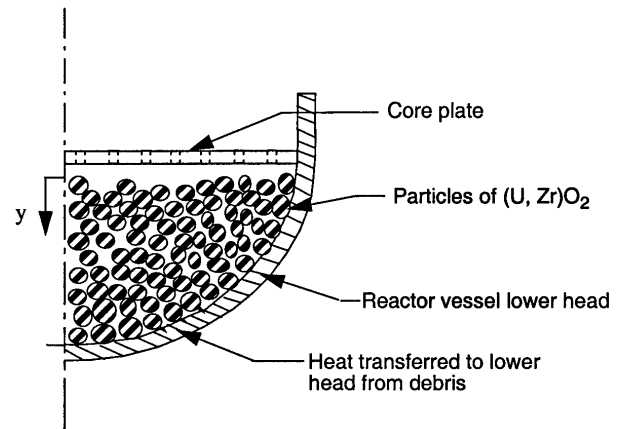


Figure 1. Schematic of debris bed in lower head of reactor vessel (particle size of debris greatly exaggerated).

accrete when molten core material slumps into a pool of water in the lower head. If the severe accident is not terminated, then eventually core plate material may melt and slump onto the top of the bed of ceramic particles. The core plate is generally composed of stainless steel and thus melts at a much lower temperature than the particles of $(\text{U}, \text{Zr})\text{O}_2$ (1700 K versus ~3000 K). The subsequent heatup of the debris bed and lower head is a function of the extent to which the melted core plate permeates into the bed of $(\text{U}, \text{Zr})\text{O}_2$ particles. This paper describes a model for calculating the permeation of the melted core plate material into the porous debris bed. Also described is the implementation of this model into the existing model in the SCDAP/RELAP5 code¹ for calculating the heatup of the debris bed and lower head supporting the debris bed.

2. MODEL FOR MOVEMENT OF MATERIAL IN POROUS DEBRIS

This section describes a model based on Darcy's Law for calculating the movement liquefied core plate material through the interstices in a matrix of porous material. A schematic of the system to be analyzed is shown in Figure 2. The movement

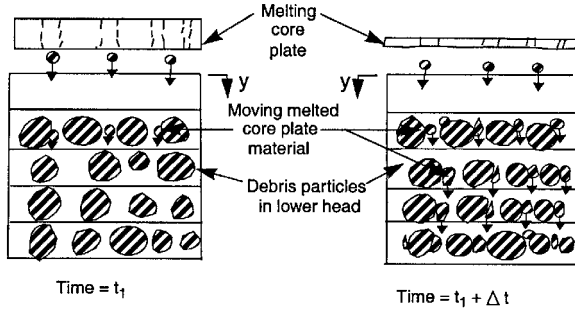


Figure 2. Schematic of movement of liquefied material within porous debris bed.

of the liquefied material is driven by several forces, including gravity, capillary force, and pressure gradient. Resistances to movement are caused by viscous forces, turbulence and form losses due to a continuous contraction and expansion of flow areas as the liquefied material flows through the porous debris. The resistances to movement increase with the velocity of the moving material. The balancing of the forces driving the movement of the liquefied material with the forces resisting the movement results in a conservation of momentum equation for the liquefied material.

Several assumptions are applied to simplify the modeling in a manner that maintains an accuracy of solution of the same order of magnitude as the uncertainties of governing material properties and debris behavior. These assumptions are: (1) the porous medium is composed only of (U, Zr)O₂ particles, (2) the material permeating the porous medium is composed only of stainless steel, (3) stainless steel does not chemically react with (U, Zr)O₂, (4) the (U, Zr)O₂ particles do not melt, (5) the permeating stainless steel is in thermal equilibrium with the (U, Zr)O₂ particles it contacts, (6) water is not present at any location with liquefied stainless steel, (7) capillary forces are negligible, (8) the frictional drag on the liquefied stainless steel is balanced by the force of gravity with the result of quasi-steady flow of the liquefied material through the voids in the debris bed (acceleration of liquefied material and momentum flux are small compared to gravity), (9) the relative passability of the debris bed is equal to its relative permeability, (10) liquefied stainless steel does not move in the radial direction; and (11) the hydrodynamic effect of a wall (lower head) on the movement of the liquefied stainless steel is negligible.

In general, the assumptions are consistent with the expected behavior of the core plate and the expected characteristics of lower plenum debris. The omission of the

inertial and capillary terms in the momentum equation is based on order of magnitude analyses.¹⁰ The expected relatively slow movement of the liquefied stainless steel justifies the assumption of thermal equilibrium between the stainless steel and the (U, Zr)O₂ matrix.¹⁰

Taking into account the above assumptions, the conservation of momentum equation for the liquefied material is given by the equation.^{2,3}

$$\frac{\mu_l j}{k_l k} + \frac{\rho_l j^2}{m_l m} = \rho_l g \quad (1)$$

where

- μ_l = dynamic viscosity (kg/m · s),
- j = superficial velocity (m/s),
- k = Darcy permeability (m²),
- k_l = relative permeability (unitless),
- m = passability of debris bed (m),
- m_l = relative passability (unitless),
- ρ_l = density (kg/m³),
- g = acceleration of gravity (9.8 m/s²).

The second term of the above equation is the turbulent drag counterpart to the viscous drag represented by the first term.

The Darcy permeability is calculated by the equation

$$k = \frac{\epsilon^3 D_p^2}{150(1 - \epsilon)^2} \quad (2)$$

where

- ϵ = porosity of the debris bed (unitless),
- D_p = diameter of particles in debris bed (m).

The passability of the debris bed is calculated by the equation

$$m = \frac{\epsilon^3 D_p}{1.75(1 - \epsilon)} \quad (3)$$

In general the relative permeability is less than the relative passability, but they are assumed to be equal for this analysis.⁴ Thus,

$$m_l = k_l \quad (4)$$

The relative permeability is a function of the effective saturation of the debris bed and the Darcy permeability. The relative permeability is calculated by the equation²

$$k_l = S_e^3 \quad (5)$$

where

- S_e = effective saturation of debris bed (unitless).

The effective saturation is calculated by the equation²

$$S_e = \frac{S - S_r}{1 - S_r} \quad (6)$$

where

S = true saturation of debris bed; volume fraction of liquefied material in pores of debris bed (unitless),

S_r = residual saturation of debris bed (unitless).

The residual saturation, S_r , is a function of the surface tension of the liquid and of the degree of wetting of the solid material by the liquefied material. Reference 2 provides an empirical equation for calculating residual saturation that is appropriate for debris resulting from the disintegration of nuclear reactor cores. This equation is

$$S_r = \begin{cases} \frac{1}{86.3} \left[\frac{\gamma \cos(\theta)}{k\rho_l g} \right]^{0.263} & ; 0 \leq \theta \leq 90^\circ \\ 0 & ; 90^\circ < \theta \leq 180^\circ \end{cases} \quad (7)$$

where

γ = surface tension of the liquid (N/m),

θ = wetting contact angle (degrees).

In the case of liquefied material that does not wet the solid material ($90^\circ < \theta < 180^\circ$), the residual saturation is equal to zero. An example of such a system is a debris bed composed of (U, Zr)O₂ and liquefied stainless steel.² In this case, bulk motion occurs at a relatively low values of bed saturation.

The conservation of mass equation is applied to obtain the relation of the rate of change with time of the local saturation of the debris bed to the local velocity of the liquefied debris. The result is the equation

$$\frac{\partial S}{\partial t} = - \frac{\partial j}{\partial y} \quad (8)$$

where

t = time (s),

y = spatial coordinate that defines elevation (defined in Figure 1) (m).

Equations (1) and (8) are a set of two equations for solving for the variables j and S . The terms k_l and m_l in Equation (1) are a function of S and thus contribute to the nonlinearity of the set of equations.

3. EFFECTS OF MATERIAL MOVEMENT ON DEBRIS BED HEAT TRANSFER

The movement of liquefied core plate material through the interstices in a porous debris bed results in the transport of energy within the debris bed. In addition, the movement of the liquefied material through the debris bed influences the thermal conductivity and heat capacity of the debris bed. As a result, the movement of liquefied material may have a significant influence on the temperature distribution within the debris bed. This section defines the heat transport equations to account for the effect of material movement on temperature distribution.

The transport of heat through a porous medium with moving material in the interstices can be calculated by the equation.^{1,10}

(9)

$$(1 - \epsilon_h)(\rho c_v)_g \frac{\partial T}{\partial t} = \frac{\partial}{\partial x} \left(k_e \frac{\partial T}{\partial x} \right) + \frac{\partial}{\partial y} \left(k_e \frac{\partial T}{\partial y} \right) + Q - \rho_l c_p j \frac{\partial T}{\partial y}$$

where

ρ = density (kg/m³),

c_v = constant volume specific heat, (J/kg · K),

k_e = effective thermal conductivity, (W/m · K),

Q = volumetric heat generation rate (W/m³),

T = temperature of debris (K),

ϵ_h = heat conduction porosity of debris;

= $\epsilon (1 - S)$ (unitless),

S = saturation of debris bed,

x = spatial coordinate in horizontal direction (m),

y = spatial coordinate in vertical direction (m),

g = subscript indicating mixture of stainless steel and (U, Zr)O₂

j = superficial velocity of liquefied material (m/s),

ρ_l = density of liquefied material (kg/m³),

c_p = heat capacity of liquefied material (J/kg · K),

$\frac{\partial T}{\partial y}$ = temperature gradient in debris bed in

direction of movement of liquefied material (K/m).

The last term in the above equation accounts for heat transport due to the flow of liquefied material through the porous debris. This term is based upon the assumption of instant thermal equilibrium of the flowing liquefied material with the debris it contacts (Assumption No. 5 in Section 2).

The movement of liquefied material through the interstices of a porous debris bed influences the effective thermal conductivity of the debris bed. The effective thermal conductivity is calculated by the equation

$$k_e = k_{ec} + k_r \quad (10) \text{ where}$$

k_e = effective conductivity (W/m · K),

k_{ec} = particle internal conductivity (W/m · K),

k_r = radiative conductivity.

The Imura-Takegoshi⁷ model for thermal conductivity is combined with the Vortmeyer⁸ radiation model.

The Imura-Takegoshi⁷ model in equation form is given as follows:

$$k_{ec} = \left[\psi + \frac{1 - \psi}{\phi + \frac{1 - \phi}{v}} \right] k_g \quad (11)$$

$$\phi = 0.3 \epsilon_h^{1.6} v^{0.044} \quad (12)$$

$$v = \frac{k_s}{k_g} \quad (13)$$

$$\psi = \frac{\varepsilon_h - \phi}{1 - \phi} \quad (14)$$

where

- k_g = thermal conductivity of vapor in pores (W/m · K),
 k_s = thermal conductivity of mixture of stainless steel and (U, Zr)O₂, (W/m · K),

- ε = porosity of debris for heat transfer calculations = ε (1-S).

The mixture thermal conductivity (k_s) is calculated by the MATPRO function named ZUTCO.⁹

The Vortmeyer model is given as

$$k_r = 4\eta\sigma D_p T^3 \quad (15)$$

where

- η = radiation exchange factor (~ 0.8),
 σ = Stefan-Boltzmann constant W/m² · K⁴ (5.668 x 10⁻⁸),
 D_p = particle diameter (m),
 T = temperature (K).

4. BOUNDARY CONDITIONS

This section describes the boundary conditions applied to the model for movement of liquefied core plate material through a ceramic porous debris bed below the core plate.

For the top of the debris bed, the equation for the velocity of the liquefied material, namely Equation (1), is replaced by the equation

$$j_T = G/\rho_l \quad (16)$$

where

- j_T = superficial velocity of liquefied material at top surface of debris bed (m/s),
 G = rate of melting of structure above debris bed per unit of cross sectional area (kg/s)/m².

When the temperature of the top surface of the debris bed is greater than the melting temperature of the core plate, then radiation heat transfer from the debris bed melts the core plate. The rate of melting at the bottom surface of the core plate is calculated by the equation

$$G = \varepsilon\sigma(T_D^4 - T_{cm}^4) / h_{fc} \quad (17)$$

where

- ε = emissivity factor,
 σ = Stefan-Boltzmann constant (5.668 x 10⁻⁸ W/m² · K⁴),
 T_D = temperature of top surface of debris (K),
 T_{cm} = melting temperature of core plate (K)
 h_{fc} = heat of fusion of core plate (J/kg).

The heat transfer at the bottom boundary of the debris bed is increased by the movement of melted core plate material to the bottom boundary. The heat transfer at the bottom

boundary is proportional to the gap heat transfer coefficient at the interface of the debris and the lower head supporting the debris. When liquefied material is not present at the interface, the gap conductance is assumed to be 500 W/m² · K. For any location on the interface that has been contacted by liquefied material, the gap heat transfer coefficient is assumed to equal 10,000 W/m² · K, which simulates the heat transfer across a gap filled with material with a relatively large thermal conductivity.

5. NUMERICAL SOLUTION

An explicit, iterative scheme is used to solve for the distribution in velocity and debris bed saturation. The coordinate system and the nodalization for the numerical solution are shown in Figure 3. The debris bed is divided into a stack of control volumes. The control volumes are connected to each other with junctions. The extent of bed saturation is calculated for each control volume and the velocity of the liquefied material is calculated at each junction. The scheme for the numerical solution is based on the concept that the velocity gradient changes at a slower rate than the degree of bed saturation. In the first step for the first iteration, the change in bed saturation for each control volume is calculated using previous time step velocities at the junctions of the control volumes. Next, the end of time step velocity at each junction is calculated using the values for bed saturation calculated in the previous step. Next, the bed saturation in each control volume is calculated using the velocities just calculated for the end of the time step. If at any control volume the difference between the last two values calculated for bed saturation is greater than the tolerance for error in bed saturation, another iteration is performed. Subsequent iterations are performed until convergence is obtained at each control volume.

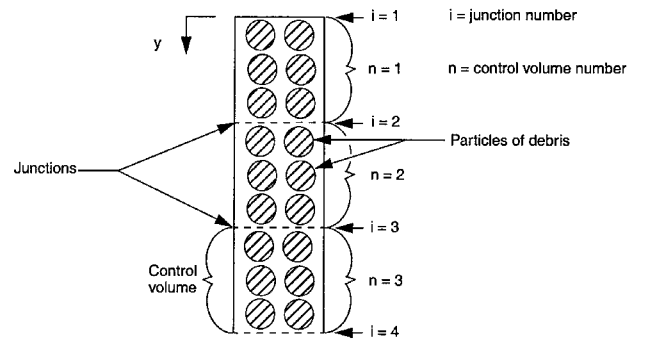


Figure 3. Coordinate system for numerical solution.

The equations in the numerical solution scheme are arranged as follows. First, a guess of the end of time step bed saturation is calculated using the equation

$$S_n^{m+1} = S_n - \left[\frac{(j_{np}^m - j_{nm}^m)}{(y_{np} - y_{nm})} \right] \Delta t \quad (18)$$

where

- m = time step number,
- S_n^{m+1} = bed saturation at control volume n at end of time step,
- S_n^m = same as S_n^{m+1} , but for start of time step,
- j_{np}^m = superficial velocity at start of time step of liquefied material at junction at downwind side of control volume n (m/s),
- j_{nm}^m = same as j_{np}^m , but for junction at upwind side of control volume n (m/s),
- y_{np} = elevation of junction at downwind side of control volume n (m),
- y_{nm} = elevation of junction at upwind side of control volume n (m),
- Δt = time step (s).

In the above equation, the control volumes are assumed to have uniform cross sectional areas.

Two categories of porosity are calculated at each control volume at each time step. One category of porosity, named the mass transport porosity, is used in the equations that calculate the flow of liquefied material. For this category, the volumes of liquid and gas are lumped together to represent the porosity. The other category of porosity, named the heat conduction porosity, is used in the equations that calculate the conduction of heat through the debris bed. For this category, the volumes of solid material and liquefied debris are lumped together.

The heat conduction porosity is related to the mass transport porosity by the equation

$$\epsilon_{hn} = \epsilon_n (1 - S_n^{m+1}) \quad (19)$$

where

- ϵ_{hn} = heat conduction porosity in control volume n (unitless),
- ϵ_n = mass transport porosity in control volume n (unitless),
- S_n^{m+1} = saturation of debris bed in control volume n (unitless).

Next, the Darcy permeability and the passability of the debris bed are updated using the equations

$$k_n = \frac{\epsilon_n^3 D_p^2}{150(1 - \epsilon_n)^2} \quad (20)$$

$$m_n = \frac{\epsilon_n^3 D_p}{1.75(1 - \epsilon_n)} \quad (21)$$

where

- k_n = Darcy permeability of debris bed at control volume n (m^2),
- m_n = passability of debris bed at control volume n (m).

Then, the effective saturation of the debris bed at the end of the time step for each control volume is calculated using the equation

$$S_{en}^{m+1} = \frac{S_n^{m+1} - S_r}{1 - S_r} \quad (22)$$

where

- S_{en}^{m+1} = effective saturation at control volume n at end of time step.

The residual saturation, S_r , is a function of material properties, namely wetting angle, surface tension, Darcy permeability, and liquid density; it is calculated using Equation 7.

Next, the relative permeability of the debris bed at the end of the time step for each control volume is calculated using the equation

$$k_{ln}^{m+1} = [S_{en}^{m+1}]^3 \quad (23)$$

where

- k_{ln}^{m+1} = relative permeability at control volume n at end of time step.

The relative passability of the debris bed at the end of the time step for each control volume is calculated using the equation

$$m_{ln}^{m+1} = k_{ln}^{m+1} \quad (24)$$

where

- m_{ln}^{m+1} = relative passability of debris bed at control volume n at end of time step.

Next, the velocity of the liquefied material at each junction is calculated using Equation (1). For numerical solution, terms in this equation are combined as follows

$$A[j_i^{m+1}]^2 + B j_i^{m+1} + C = 0 \quad (25)$$

where

- j_i^{m+1} = superficial velocity at junction i at end of time step (m/s),
- $A = \frac{\rho_l}{m_{li}^{m+1} m_i}$
- $B = \frac{\mu_l}{k_{li}^{m+1} k_i}$
- $C = -\rho_l g$
- ρ_l = density of liquefied debris (kg/m^3),
- μ_l = dynamic viscosity of liquefied material ($kg/m \cdot s$),
- g = acceleration of gravity ($9.8 m/s^2$),
- m_{li}^{m+1} = relative passability at junction i at end of time step (unitless),
- k_{li}^{m+1} = relative permeability at junction i at end of time step (unitless).

The relative permeability and passability at junction i are defined to be the average of the values of these variables at the two control volumes upwind and downwind of junction i .

Applying the quadratic equation, the superficial velocity of the liquefied material at each node at the end of the time step is calculated using the equation

$$j_i^{m+1} = \frac{-B \pm [B^2 - 4AC]^{0.5}}{2A} \quad (26)$$

The above equation has two values. Since the liquefied material can only flow down, only the positive value is applied.

At the top junction in the debris bed, the superficial velocity is calculated by the equation

$$j_1 = G / \rho_1 \quad (27)$$

where

j_1 = superficial velocity at top junction in debris bed (m/s),

G = rate of melting of structure above the debris bed per unit of cross sectional area (kg/s)/m².

At the bottom junction, the boundary condition corresponding with an impermeable boundary is imposed. Thus, $j_{nb} = 0.0$ (28)

where

j_{nb} = superficial velocity at bottom most junction in debris bed (m/s).

The bed saturation in each control volume at the end of the time step is then calculated using Equation (18) with the start of time step superficial velocities in this equation replaced with the end of time superficial velocities calculated by Equation (26).

The fractional difference in bed saturation between two successive iterations is calculated by the equation

$$f_n = \frac{S_n^{r+1} - S_n^r}{0.5(S_n^{r+1} + S_n^r)} \quad (29)$$

where

f_n = fractional difference in value of S_n^{m+1} between two successive iterations,

r = iteration number,

S_n^r = value of S_n^{m+1} at r -th iteration.

If the value of f_n at any control volume is greater than the tolerance in error for bed saturation, another iteration is performed. The results of a sensitivity study indicated that a value for the tolerance in error of 0.001 is appropriate.¹⁰

After convergence of the debris bed saturation at each control volume has been obtained, the effect of the movement of liquefied material during the time step on heat transport is calculated. First, the effect of the movement of liquefied material on heat transport is accounted for by evaluating the last term in Equation 9. Then, the heat conduction porosity for each control volume is updated to account for the addition or subtraction of material from each control volume during the

time step. Then, the volume fractions of metallic material and (U, Zr)O₂ at each control volume are updated to account for the addition or subtraction of material from each control volume during the time step.

6. APPLICATION TO SEVERE ACCIDENT IN PWR

The model for movement of liquefied material through porous debris was implemented into the SCDAP/RELAP5 code¹⁰ and applied to the analysis of the heatup of a debris bed situated below a core plate. A schematic of the system analyzed is shown in Figure 4. The analysis has application to the evaluation of the structural integrity of the lower head. If the heat flux on the external surface of the lower head does not exceed the critical heat flux, then the structural integrity of the lower is more likely to be retained.

In the assumed severe accident situation in a PWR, a 0.9 m deep porous debris bed is resting on the inner surface of the lower head of the reactor vessel. Decay heat in the debris has boiled all water out of the vessel. As a result, the vessel is filled with steam at a pressure of 0.2 MPa. Heat radiating from the top surface of the debris bed is melting the bottom of the stainless steel core plate located above the debris bed. The melted core plate material is slumping to the top of the debris bed and then permeating into the debris bed. The dashed lines in Figure 4 describe the finite elements and control volumes used in the numerical solution to represent the debris, lower head, and the core plate material permeating the debris. The intersections of the dashed lines are the nodes at which temperature was calculated. The bottom of the debris bed interfaces with the inner surface of the lower head. The outer surface of the lower head is in contact with a pool of water. The initial conditions and boundary conditions are summarized in Table 1. The initial temperature of the debris bed is 1727 K, which corresponds with the liquidus temperature of the core plate. The entire lower head is assumed to have an initial temperature of 400 K. The debris has an internal heat generation rate due to decay heat in the UO₂ of 1 MW/m³. The debris bed has a porosity of 0.4 and is composed of UO₂ particles with a diameter of 3 mm. The analysis starts at a time of 0.0 s.

The melted core plate material is calculated to permeate to within 0.05 m of the bottom of the debris bed. Figure 5 is a plot of the axial distribution in debris bed saturation and temperature along its centerline for the time of 1500 s, when 30% of the core plate was calculated to have melted and slumped onto the debris bed. In general, the liquefied stainless steel was calculated to move downward through the debris at a

Table 1. Initial conditions and boundary conditions.

Characteristic	Value
core plate material	stainless steel
mass of core plate (kg)	25,000

debris bed material	UO ₂
debris bed porosity	0.4
maximum depth of debris bed (m)	0.9
initial temperature of debris bed (K)	1727
nuclear heat generation rate in debris bed (MW/m ³)	1
diameter of particles in debris bed (mm)	3
initial temperature of lower head of reactor vessel (K)	400
thickness of lower head (m)	0.158
composition of lower head	carbon steel
heat transfer coefficient at interface of debris and lower head (W/m ² .K)	500

rate of about 2 mm/s. Due to the cold temperature of the debris near the lower head, a crust of frozen core plate material formed about 0.05 m above the surface of the lower head. Above this crust, an ever increasing region of the debris bed was calculated to become saturated with core plate material. At 2000 s, when 50% of the core plate was calculated to have melted, a 0.2 m deep region along the centerline of the debris bed was calculated to be saturated.

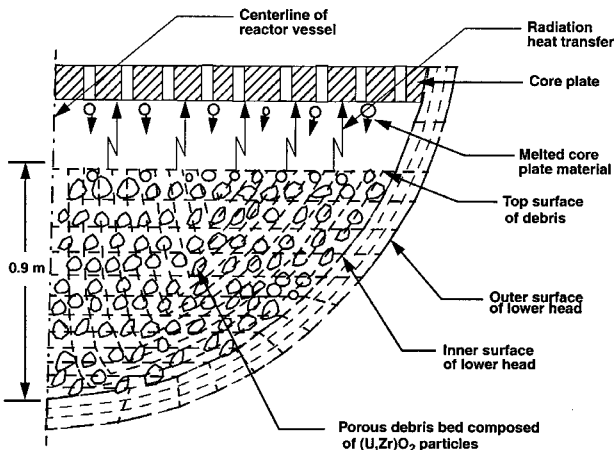


Figure 4. Schematic of system analyzed and nodalization of system.

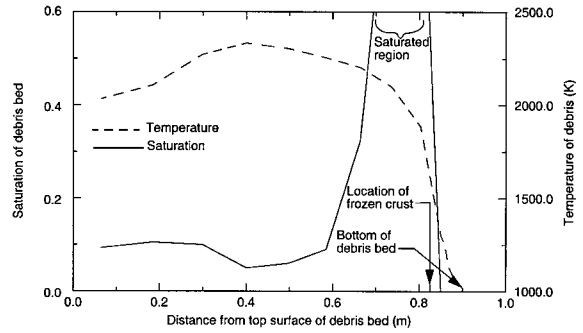


Figure 5. Distribution of debris bed saturation and temperature after melting of 30% of core plate (time of 1500 s).

The temperature of the debris bed was calculated to continually increases with time due to inadequate cooling. The calculated transient temperature distribution in the debris bed is plotted in Figure 6 for two locations along the centerline of the debris bed. The first location is at the top of the debris bed and the second location is 0.7 m below the top of the debris bed. At the location 0.7 m below the top surface, the temperature of the debris was calculated to increase at a rate of 0.35 K/s. The temperature of the location at the top surface was calculated to increase at a slower rate due to contact with the relatively cool liquefied core plate material and due to convective and radiative cooling. At 2500 s, the temperatures of these two locations were calculated to be 2115 K and 2540 K, respectively.

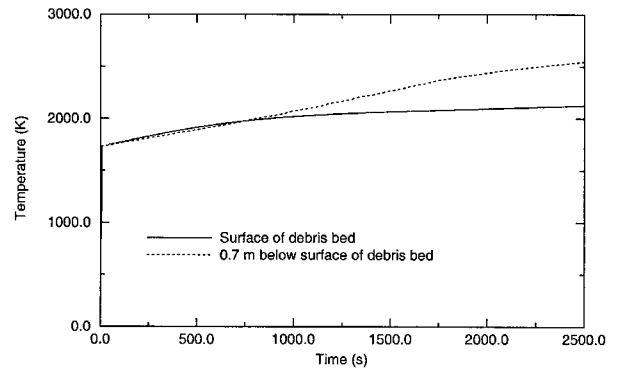


Figure 6. Temperature history of debris bed along its centerline.

The permeation of core plate material into the porous debris bed did not significantly increase the heat flux on the external surface of the lower head. Plots of the ratio of heat flux to critical heat flux (CHF) at the bottom center of the lower head for the cases of core plate material permeating through the debris bed and core plate material staying above the debris are compared in Figure 7. Generally, the value of

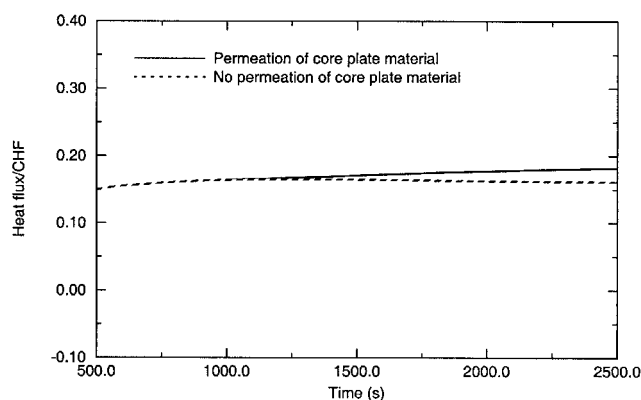


Figure 7. Ratio of heat flux to CHF on external surface at bottom center of lower head.

CHF is smallest at the bottom center. As shown in this figure, the heat flux ratios for the two cases are nearly equal until 1000 s, after which the heat flux ratio becomes greater for the case of core plate material permeating through the debris bed. At 2500 s, when 66% of the core plate was calculated to have melted and permeated into the debris bed, the heat flux ratio for the case of core plate permeation was calculated to be about 12% greater than for the case without permeation. The somewhat higher heat flux for the case with permeation is due to the increase in effective thermal conductivity caused by the presence of core plate material in the debris. The calculated effective thermal conductivity for three levels of debris saturation are shown in Table 2. The effective thermal conductivity ranges from 2.5 W/m · K for a saturation value of zero to 9.4 W/m · K for fully saturated debris. This increase in thermal conductivity of the debris increases the rate of heat transfer from the interior of the debris to the lower head supporting the debris. Nevertheless, the heat flux is considerably less than the critical heat flux even for the case of permeation of core plate material into the debris bed.

Table 2. Effect of level of debris saturation on thermal conductivity of debris.

Level of debris saturation	Effective thermal conductivity (W/m.K)
0.0	2.5
0.20	4.7
1.0	9.4

7. CONCLUSIONS

The structural integrity during a severe accident of the lower head of a PWR may be influenced by the extent to which melted core plate material permeates into porous core debris supported by the lower head. A model based on Darcy's Law has been developed for calculating the permeation of liquefied core plate material through porous debris. This model was

implemented into the severe accident analysis code named SCDAP/RELAP5 and combined with a model for two-dimensional heat transport in porous debris. These two models provide the capability to calculate the rate of melting of a core plate above debris in the lower head, and to calculate the subsequent influence of the melted and slumped core plate material on the heatup of the debris and lower head. Calculations with the models indicate that, for the case of a core plate above a 0.9 m deep debris bed with an internal heat generation rate of 1 MW/m³, 50% of the core plate would melt due to radiation heat transfer from the surface of the debris in the 2000 s period of time after heatup of the debris to the melting temperature of the core plate. The calculations also indicate that core plate material may permeate to near the bottom of a porous debris bed in the lower head. Permeation to the inner surface of the lower head was calculated to be blocked by freezing of the core plate material. The permeation of core plate material into the debris increased the effective thermal conductivity of the debris, and, as a result, the heat flux at the external surface of the lower head was calculated to be about 12% greater than the case without permeation. Nevertheless, the maximum heat flux was calculated to be significantly less than the critical heat flux.

8. ACKNOWLEDGEMENTS

Work supported by the U.S. Nuclear Regulatory Commission under DOE Idaho Operations Office Contract DE-AC07-99ID13727.

9. REFERENCES

1. The SCDAP/RELAP5 Development Team, "SCDAP/RELAP5/MOD3.2 Code Manual, Volume 2: Damage Progression Model Theory," NUREG/CR-6150, Volume 2, Rev. 1, INEL-96/0422, July 1998.
2. R. C. Schmidt and R. D. Gasser, "Models and Correlations of the DEBRIS Late-Phase Melt Progression Model," SAND93-3922, September 1997.
3. L. J. Siefken, "SCDAP/RELAP5 Modeling of Movement of Melted Material Through Porous Debris in Lower Head," INEEL/EXT-98-01178, December 1998.
4. Mo Chung and Ivan Catton, "Post-Dryout Heat Transfer in a Multi-Dimensional Porous Bed," Nuclear Engineering and Design 128 (1991) pages 289-304.
5. F. B. Cheung, K. H. Haddad, and Y. C. Liu, "A Scaling Law for the Local CHF on the External Bottom Side of a Fully Submerged Reactor Vessel," NUREG/CP-0157, Vol. 2, February 1997, pp. 253-277.
6. The RELAP5 Development Team, "RELAP5 Code Manual, Models and Correlations," NUREG/CR-5535, Vol. 4, August 1995.
7. S. Imura and E. Takegoski, "Effect of Gas Pressure on the Effective Thermal Conductivity of Packed Beds," Heat Transfer Japanese Research, 3, 4, 1974, p. 13.

8. D. Vortmeyer, "Radiation in Packed Solids," 6th International Heat Transfer Conference, Toronto, Canada, 1978.
9. The SCDAP/RELAP5 Development Team, "SCDAP/RELAP5/MOD3.2 Code Manual, Volume 4: MATPRO - A Library of Materials Properties for Light-Water-Reactor Accident Analysis," NUREG/CR-6150, Volume 4, Rev. 1, INEL-96/0422, July 1998
10. L. J. Siefken, "SCDAP/RELAP5 Modeling of Movement of Melted Material Through Porous Debris in Lower Head," INEEL/EXT-98-01178 Rev. 2, October 1999.
11. T. G. Theofanous, C. Liu, S. Additon, S. Angelini, O. Kymalaen, and T. Salmassi, "In-Vessel Coolability and Retention of Core Melt," DOE/ID-10460, Vol. 1, July 1995.